ISSN 1068-3356, Bulletin of the Lebedev Physics Institute, 2023, Vol. 50, No. 3, pp. 97–102. © Allerton Press, Inc., 2023.
Russian Text © The Author(s), 2023, published in Kratkie Soobshcheniya po Fizike, 2023, Vol. 50, No. 3, pp. 31–39.

Anomaly in Pyroelectric Current Generation with Varying Lithium Tantalate Single Crystal Temperature with a Constant Rate

M. E. Gilts[a], I. A. Kishin[a,b], A. A. Klenin[a], A. S. Kubankin[a,b], and A. N. Oleinik[a,*]

[a] *Laboratory of Radiation Physics, Belgorod State University, Belgorod, 308015 Russia*

[b] *Lebedev Physical Institute, Russian Academy of Sciences, Moscow, 119991 Russia*

**e-mail: oleynik_a@bsu.edu.ru*

Received November 2, 2022; revised January 31, 2023; accepted February 1, 2023

Abstract—Recently, it was established that the X-ray generation intensity increases in a certain range of temperature variation rates (6–8°C/min) of lithium tantalate single crystal ($LiTaO_3$). In this work, the pyroelectric current generation is studied as a function of the temperature variation rate. Four stages of the pyroelectric current generation dynamics are determined. In the same rate range (6–8°C/min), an anomalously long stage of current saturation is observed, which is most likely the cause of the observed effect of an increase in the X-ray intensity. The observed anomaly is described, as well as systematic features in the pyroelectric current dynamics with varying the pyroelectric material temperature with a constant rate.

Keywords: lithium tantalate, pyroelectric effect, heat propagation in solid, dielectrics

DOI: 10.3103/S1068335623030041

1. INTRODUCTION

The pyroelectric effect is unique in the fact that it in essence relates electrical and thermal properties of an individual material and makes it possible to control one property via another. Currently, the pyroelectric effect is known in both natural minerals [1] and in synthesized materials (bulk single crystals [2, 3], ceramics [4], polymers [5], two-dimensional films [6]). The possibility of generating electricity due to a very small change in the temperature has found application in infrared radiation flux detection [7, 8] and in image converters [9]. Recently, the direction of compact electrogenerators and energy storage devices based on the pyroelectric effect [10–13] are actively developed. It should also be noted that the pyroelectric effect implementation for lithium niobate and lithium tantalate single crystals [14], as well as zirconate-lead titanate ceramics [15, 16] under conditions of ambient vacuum leads in the generation of a strong electric field and generation of various particles [14, 17, 18] (electrons, positive ions, X-ray photons and neutrons), which makes it promising to develop accelerators and deflectors based on the pyroelectric effect [19, 20]. Such promising application prospects make relevant a detailed study of the interrelation between the thermal exposure of a pyroelectric material and a subsequent electrical response.

A prominent example of the effect of the interrelation of electrical and thermal properties of pyroelectrics is the existence of the optimum temperature variation rate of the piroelectric crystal, at which the intensity of generated X-rays in the pyroelectric accelerator is maximum [21]. It was shown that a peak value of the X-ray intensity is observed at the temperature variation rate of the lithium tantalate single crystal in the range of 6–8°C/min in comparison with other temperature variation rates (the range of temperature variation rates is 0.5–24°C/min; therewith, the temperature variation range was identical to each measurement). Thus, the temperature variation parameters of a pyroelectric material have a significant effect on not only the primary electrical response, but also on secondary processes.

This work is devoted to a more detailed study of the effect of the temperature variation rate of the lithium tantalate ($LiTaO_3$) single crystal exactly on the electrical response manifesting itself as pyroelectric current generation. Four stages of the pyroelectric current dynamics are determined, whose manifestation and duration are controlled by the temperature variation rate of a pyroelectric material. It was shown that anomalously long pyroelectric current generation at a high level is observed exactly in the range of 6–8°C/min, which does cause the previously observed effect of increasing the X-ray intensity.

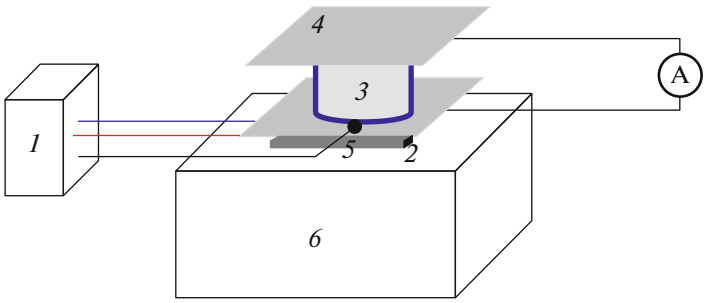

Fig. 1. Scheme for measuring the pyroelectric current with varying lithium tantalate single crystal temperature with a constant rate.

2. EXPERIMENTAL TECHNIQUE

Figure 1 shows the scheme for measuring the pyroelectric current with lithium tantalate single crystal temperature varying with a constant rate. An assembly of a pyroelectric sample *3*, two aluminum foils *4* covering polar single crystal surfaces, a Peltier element *2*, and a metal radiator *6* was joined using EPOXY H21D conductive glue. The entire assembly was placed into a metal chamber to avoid external interference. Both aluminum foils 22 × 22 mm in size were connected in series to a picoamperemeter. Thus, the pyroelectric sample can be presented as a capacitor, and the induced pyroelectric current is a capacitor discharge current. The temperature was varied with a constant rate using a temperature regulator *1* supplying the Peltier element; in this case, the supplied power was adjusted according to indications of a thermocouple *5* placed at the $LiTaO_3$ crystal base. The average background current in the circuit (the background current is a circuit current when the single crystal is in the thermodynamic equilibrium state) did not exceed 1.5 pA (the pyroelectric current level is several to tens of nA). The effect of contact phenomena between the foil, glue, and single crystal surface was not observed. The used epoxy glue has an excellent electric and thermal conductivity, which allows neglecting the heat loss and circuit current loss because of its use. The used samples of the Z-oriented single-domain lithium tantalate single crystal were prepared at the Tananaev Institute of Chemistry and Technology of Rare Elements and Mineral Raw Materials, Kola Science Center, Russian Academy of Sciences, Apatity, Russia. The samples were shaped as cylinders 10 mm high and 20 mm in diameter. The temperature regulator was developed by the Marathon Open Company (Russia), the supply parameters of the Peltier element are varied by a proportional—integral—differential (PID) PID-controller. The pyroelectric current was measured using a Keithley 6485 single-channel picoammeter.

To compare the generated current parameters at various temperature variation rates, identical experimental conditions should be provided, in particular, measurements should be performed in the same temperature variation range of the pyroelectric sample. This allows for the identical charge generated in each measurement and correct comparison of different temperature variation rates without regard to the effect of the temperature difference itself.

In all performed measurements, the temperature variation range was fixed, 15°C. Upon heating, the temperature was varied from 28.0 ± 1.0°C to 43.0 ± 1.0°C; upon cooling, the temperature was varied from 31.0 ± 1.0°C to 16.0 ± 1.0°C. Accordingly, the acquisition time t_{acq} at various temperature variation rates was different and depended on the rate:

$$t_{acq} = 15/\frac{d(\Delta T)}{dt}. \quad (1)$$

Upon heating, measurements were performed at variation rates in the range of 2–22°C/min; upon cooling, at 2–10°C/min with a step of 2°C/min. At each point, three independent measurements upon heating and cooling of the pyroelectric sample were performed; in this case, the rate holding error did not exceed 0.4°C/min.

Thus, the electric current generation upon heating and cooling of lithium tantalate samples was studied at a fixed temperature variation range and various temperature variation rates.

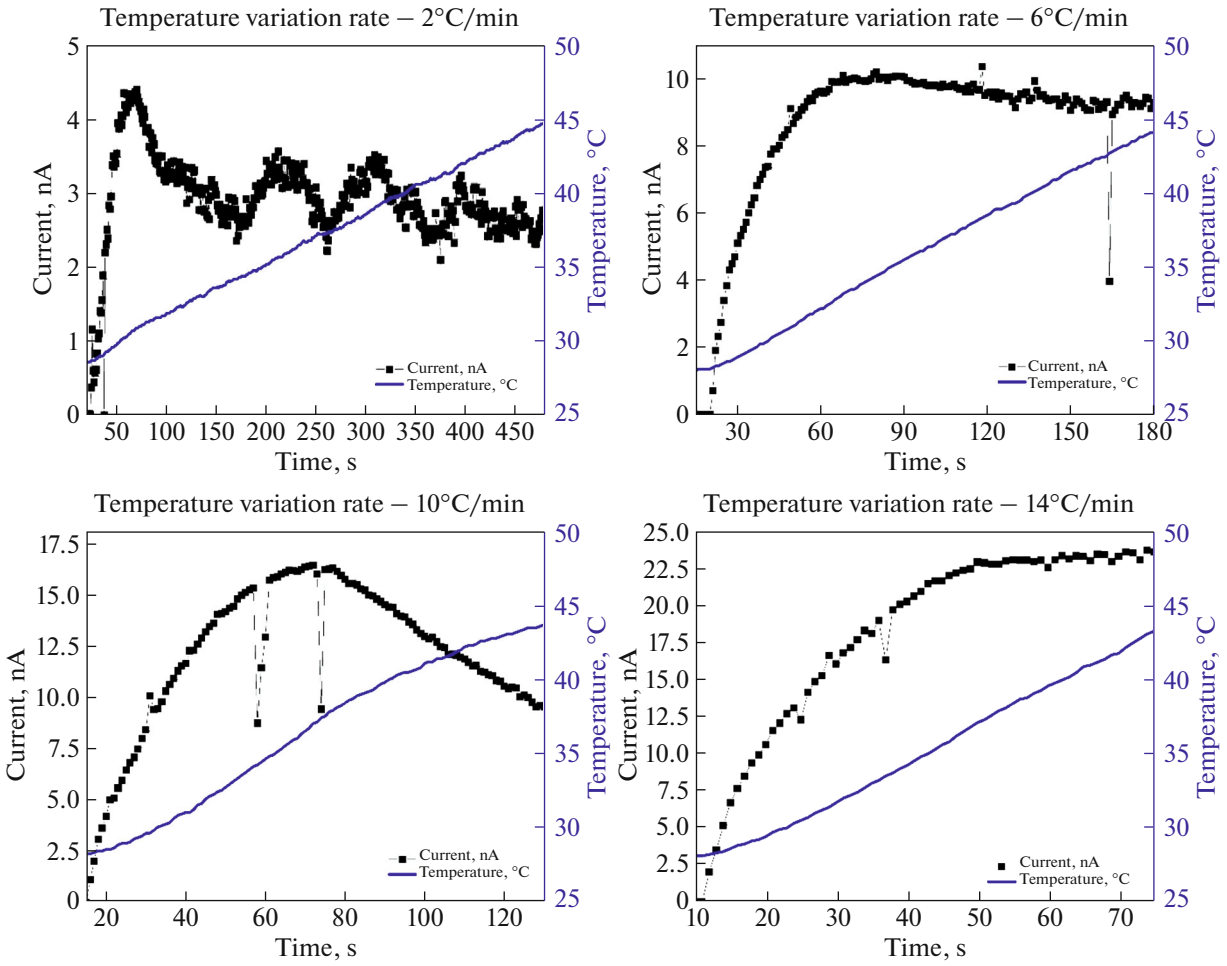

Fig. 2. Electric current curves and thermocouple readings measured during lithium tantalate sample heating with various rates. (The rate is indicated over each curve.)

3. RESULTS AND DISCUSSION

Figure 2 shows the electric current curves measured at various heating rates (2, 6, 10, 14°C/min). Four types of generated current curves can be distinguished, which are defined by the temperature variation rate and the thermal exposure duration. The first curve type appears at low temperature variation rates (to 4°C/min). In this case, the measured current curve can be divided into four stages of current generation dynamics. For example, in the case of 2°C/min, the first 60 s is the pyroelectric current increase stage, the second stage ($t = 60–80$ s) is the pyroelectric current saturation and leveling, the third stage is a decrease in the pyroelectric current level ($t = 80–150$ s), and the fourth stage is current oscillations ($t = 150–480$ s) with an amplitude to 1 nA mostly toward increasing the current level with a period to 90 s.

The second curve type appears at rates above 8°C/min and below 12°C/min. In this case, there is no last stage of current oscillations. The third curve type takes place in the range of 6–8°C/min; there is no stage of decreasing the generated current level, and the stage of generated current saturation lasts 100–120 s instead of 20 s. The fourth curve type takes place at a temperature variation rate above 12°C/min; it includes only the first growth stage and the saturation stage 15–20 s long.

Noteworthy is the fact that the stage does not disappears sequentially with increasing temperature variation rate (or, what is the same under experimental conditions, with decreasing thermal exposure duration). In the range of 6–8°C/min, the third stage of decreasing generated current level is absent; at a higher rate, 8–12°C/min, the above-mentioned stage takes place.

Thus, the shape of the generated current curve depends on the temperature variation rate, and the dependence is nontrivial and is associated not only with that the variation duration decreases.

Another interesting feature is that the first stage of an active increase in the generated current lasts the same time of 60 ± 5 s, independently of the set temperature variation rate of the sample. Most likely this

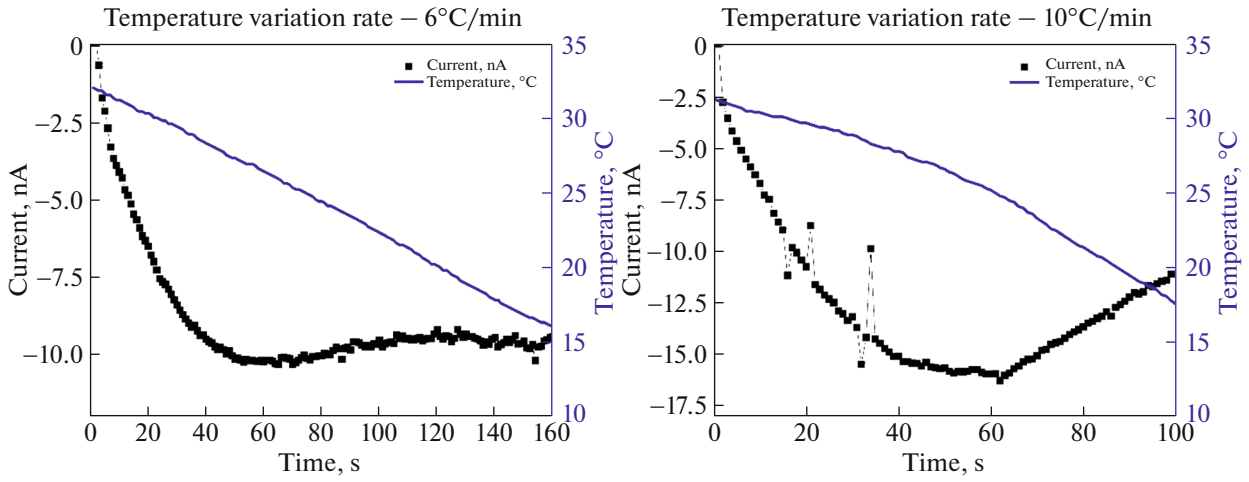

Fig. 3. Electric current curves and thermocouple readings measured upon lithium tantalite sample cooling with various rates. (The rate is indicated over each curve.)

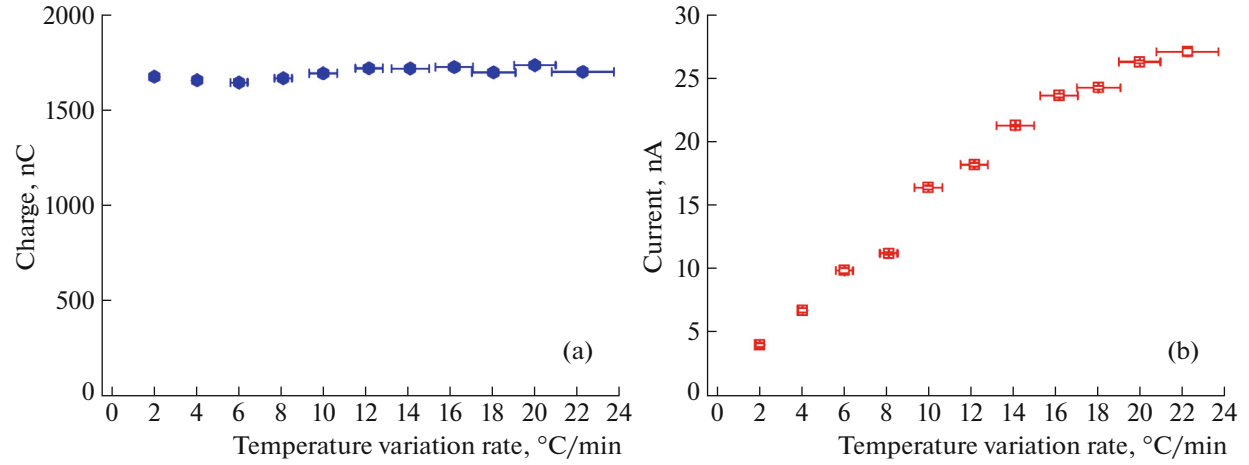

Fig. 4. (a) Charge measured during sample heating as a function of the temperature variation rate, (b) dependence of the saturation current on the temperature variation rate during sample heating.

value related to the pyroelectric sample thickness and features of the propagation of the thermal excitation within a sample and corresponding electrical response [2]. The nature of the final oscillation stage at low temperature variation rates is not entirely clear. It is possible that this phenomenon can be associated with an increase in the effect of the heat loss through crystal side surfaces, which causes an additional transverse temperature gradient and initiates the tertiary pyroelectric effect associated with the inhomogeneous temperature distribution [22].

The study of the current generation dynamics upon cooling lithium tantalite sample was limited by the capability of the used Peltier element and radiators. However, the measurements performed upon cooling to a rate of 10°C/min was sufficient to distinguish the same features in the case of coolings as well.

Figure 3 shows the electric current curves and thermocouple readings upon cooling of the sample (the rate is 6 and 10°C/min). The absence of the stage of generated current level drop and a larger stage of generated current saturation in the range of 6–8°C/min are also observed upon cooling. As the temperature variation rate increases, the current drop stage appears again. Thus, this feature remains in force upon cooling of the sample as well and is an essential feature which appears independently of the thermal exposure type and the polarity of the charge induced on the surface.

The identical temperature variation range in all measurements resulted in that about the same generated charge was recorded independently of the temperature variation rate and measurement time, which is shown in Fig. 4a. This circumstance is completely explained by the pyroelectric effect nature. At the same time, the generated electric current is directly proportional to the temperature vari-

ation rate; Fig. 4b shows the dependence of current in the saturation stage on the temperature variation rate. The current linearly increases the temperature variation rate up to 16°C/min (except for the deviation near the region of 8°C/min, which does provide the observed anomaly.

Thus, the detected electric current generation dynamics nontrivially depends on the pyroelectric temperature variation rate, although the entire observed pattern does not contradict pyroelectric effect physics. For now, the question remains open what is the mechanism of a strong increase in the duration of the generated current saturation stage and a simultaneous decrease in the saturation current in this stage in the range of the temperature variation rate of 6–8°C/min. Most likely, exactly this effect does lead to the existence of optimum conditions for a temperature change for generating strong electric fields and accompanying effects of particle generation.

4. CONCLUSIONS

The experimentally studied dependence of the pyroelectric current dynamics on the temperature variation rate of the lithium tantalate sample at a constant temperature variation range is presented in this paper.

It was found that there are four stages of the pyroelectric current dynamics with constant-rate varying temperature: the current growth stage, the saturation stage, the decrease stage, and slow oscillations about a certain nonzero value. All four stages are observed only at low temperature variation rates (to 2°C/min).

In the range of 6–8°C/min, both upon heating and upon cooling, an anomaly in the pyroelectric current dynamics is observed, which consists in a longer stage of current saturation in comparison with other temperature variation rates. We note that the observed anomaly has an effect on the pyroelectric effect manifestation and accompanying phenomena. In particular, exactly in this range of 6–8°C/min of the temperature variation rates for lithium tantalate samples of similar geometry, a strong increase in the X-ray intensity was observed when using the sample in the pyroelectric accelerator [21]. The observed anomaly can also find applications for compact electrogenerators, energy storage and conversion devices based on the pyroelectric effect.

FUNDING

This paper was prepared within the development program of the National Research University Belgorod State University for 2021–2030 (“Priority-2030” program of strategic academic leadership). The work of one of the authors (A.N.O.) was supported supported by the Russian Science Foundation, project no. 21-72-00006.

CONFLICT OF INTEREST

The authors declare that they have no conflicts of interest.

REFERENCES

1. Bruster, D., *Edinburgh Journal of Science*, Edinburgh: William Blackwood, 1824, vol. 1.
2. Bush, A.A., *Pyroelectric Effect and Its Applications*, Moscow: MIREA, 2005.
3. Tagantsev, A.K., Pyroelectric, piezoelectric, flexoelectric, and thermal polarization effects in ionic crystals, *Sov. Fiz. Usp.*, 1987, vol. 30, no. 7, p. 588. https://doi.org/10.1070/PU1987v030n07ABEH002926
4. Lang, S.B., Rice, L.H., and Shaw, S.A., Pyroelectric effect in barum titanate ceramic, *J. Appl. Phys.*, 1969, vol. 40, p. 4335. https://doi.org/10.1063/1.1657195
5. Furukawa, T., Piezoelectricity and pyroelectricity in polymers, *IEEE Trans. Electric. Ins.*, 1989, vol. 24, no. 3, p. 375. https://doi.org/10.1109/14.30878
6. Zook, J.D. and Liu, S.T., Pyroelectric effects in thin film, *J. Appl. Phys.*, 1978, vol. 49, p. 4604. https://doi.org/10.1063/1.325442
7. InfraTec, Pyroelectric Infrared Detectors. https://www.infratec-infrared.com/sensor-division/service-glossary/pyroelectric-detector/
8. Dias, Pyroelectric Infrared Detectors. http://www.dias-infrared.de/pdf/basics_eng.pdf
9. Goncharenko, B.G., Bryukhnevich, G.I., and Olikhov, I.M., Pyroelectric image converter (versions), RF Patent 2160479, 1995.

10. Zabek, D., Taylor, J., Ayel, V., Bertin, Y., Romestant, C., and Bowen, C.R., A novel pyroelectric generator utilising naturally driven temperature fluctuations from oscillating heat pipes for waste heat recovery and thermal energy harvesting, *J. Appl. Phys.*, 2016, vol. 120, p. 024505
https://doi.org/10.1063/1.4958338
11. Zhao, T., Jiang, W., Liu, H., Niu, D., Li, X., Liu, W., and Lu, B., An infrared-driven flexible pyroelectric generator for non-contact energy harvester, *Nanoscale*, 2016, vol. 8, pp. 8111—8117.
https://doi.org/10.1039/C5NR09290F
12. Sultana, A., Alam, M.M., Middya, T.R., and Mandal, D., A pyroelectric generator as a self-powered temperature sensor for sustainable thermal energy harvesting from waste heat and human body heat, *Applied Energy*, 2018, vol. 221, pp. 299—307.
https://doi.org/10.1016/j.apenergy.2018.04.003
13. Thakre, A., Kumar, A., Song, H.C., Jeong, D.Y., and Ryu, J., Pyroelectric energy conversion and its applications—Flexible energy harvesters and sensors, *Sensors*, 2019, vol. 19, p. 2170.
https://doi.org/10.3390/s19092170
14. Brownridge, J.D., *Trends in Electro-Optics Research*, New York: Nova Science, 2005.
15. Shchagin, A.V., Miroshnik, V.S., Volkov, V.I., and Oleinik, A.N., Ferroelectric ceramics in a pyroelectric accelerator, *Appl. Phys. Lett.*, 2015, vol. 107, p. 233505.
https://doi.org/10.1063/1.4937007
16. Oleinik, A.N., Bolotov, E.V., Gilts, M.E., Ivashchuk, O.O., Klenin, A.A., Kubankin, A.S., and Shchagin, A.V., Dependence of the endpoint energy of X-ray radiation on the preliminary temperature change during the pyroelectric source operation in the pulsed mode, *Bull. Lebedev Phys. Inst.*, 2021, vol. 48, pp. 127—130.
17. Brownridge, J.D. and Shafroth S.M., X-ray fluoresced high-Z (up to $Z = 82$) K X-rays produced by $LiNbO_3$ and $LiTaO_3$ pyroelectric crystal electron accelerators, *Appl. Phys. Lett.*, 2004, vol. 85, p. 1298.
https://doi.org/10.1063/1.1782260
18. Naranjo, B., Gimzewski, J., and Putterman, S., Observation of nuclear fusion driven by a pyroelectric crystal, *Nature*, 2005, vol. 434, pp. 1115—1117.
https://doi.org/10.1038/nature03575
19. Ghaderi, R. and Davani, F.A., Dynamics of pyroelectric accelerators, *Appl. Phys. Lett.*, 2015, vol. 106, p. 042906.
https://doi.org/10.1063/1.4906866
20. Oleinik, A.N., Kubankin, A.S., Nazhmudinov, R.M., Karataev, P.V., Shchagin, A.V., and Vokhmyanina, K.A., Pyroelectric deflector of charged particle beam, *J. Instrum.*, 2016, vol. 11, p. 08007.
https://doi.org/10.1088/1748-0221/11/08/P08007
21. Kubankin, A.S., Chepurnov, A.S., Ivashchuk, O.O., Ionidi, V.Yu., Kishin, I.A., Klenin, A.A., Oleinik, A.N., and Shchagin, A.V., Optimal speed of temperature change of a crystal in a pyroelectric X-ray radiation source, *AIP Advances*, 2018, vol. 8, p. 035207.
https://doi.org/10.1063/1.5006486
22. Kosorotov, V.F., Kremenchugskij, L.S., Levash, L.V., and Shchedrina, L.V., Tertiary pyroelectric effect in lithium niobate and lithium tantalate crystals, *Ferroelectrics*, 1986, vol. 70, p. 27.
https://doi.org/10.1080/00150198608221418

Translated by A. Kazantsev